HHS Public Access

Author manuscript

Gastroenterology. Author manuscript; available in PMC 2018 September 01.

Published in final edited form as:

Gastroenterology. 2017 September ; 153(3): 753–761. doi:10.1053/j.gastro.2017.06.005.

Agreement Between Magnetic Resonance Imaging Proton Density Fat Fraction Measurements and Pathologist-assigned Steatosis Grades of Liver Biopsies from Adults with Nonalcoholic Steatohepatitis

Michael S. Middleton, MD, PhD[1], **Elhamy R. Heba, MD**[1], **Catherine A. Hooker, BSc**[1], **Mustafa R. Bashir, MD**[2], **Kathryn J. Fowler, MD**[3], **Kumar Sandrasegaran, MD**[4], **Elizabeth M. Brunt, MD**[3], **David E. Kleiner, MD, PhD**[5], **Edward Doo, MD**[6], **Mark L. Van Natta, MHS**[7], **James Tonascia, PhD**[7], **Joel E. Lavine, MD, PhD**[8], **Brent A. Neuschwander-Tetri, MD**[3], **Arun Sanyal, MD**[9], **Rohit Loomba, MD, MHSc**[10], and **Claude B. Sirlin, MD**[1] **for the NASH Clinical Research Network**

Corresponding author contact information: Michael S. Middleton, MD PhD, Liver Imaging Group, Department of Radiology, UCSD School of Medicine, 408 Dickinson Street, San Diego, CA 92103-8226, msm@ucsd.edu.

Author contributions: Michael S. Middleton, MD PhD study concept and design acquisition of data analysis and interpretation of data drafting of manuscript critical revision of manuscript for important intellectual content study supervision
Elhamy R. Heba, MD analysis and interpretation of data drafting of manuscript critical revision of manuscript for important intellectual content
Catherine A. Hooker, BSc analysis and interpretation of data drafting of manuscript critical revision of manuscript for important intellectual content
Mustafa Bashir, MD acquisition of data analysis and interpretation of data drafting of manuscript critical revision of manuscript for important intellectual content
Kathryn J. Fowler, MD acquisition of data analysis and interpretation of data drafting of manuscript critical revision of manuscript for important intellectual content
Kumar Sandrasegaran, MD acquisition of data analysis and interpretation of data drafting of manuscript critical revision of manuscript for important intellectual content
Elizabeth M. Brunt, MD analysis and interpretation of data drafting of manuscript critical revision of manuscript for important intellectual content
David E. Kleiner, MD PhD analysis and interpretation of data drafting of manuscript critical revision of manuscript for important intellectual content
Edward Doo, MD study concept and design obtained funding drafting of manuscript critical revision of manuscript for important intellectual content
Mark L. Van Natta, MHS analysis and interpretation of data drafting of manuscript critical revision of manuscript for important intellectual content statistical analysis
James Tonascia, PhD study concept and design analysis and interpretation of data drafting of manuscript critical revision of manuscript for important intellectual content study supervision obtaining funding statistical analysis
Joel E. Lavine, MD, PhD study concept and design drafting of manuscript critical revision of manuscript for important intellectual content obtaining funding
Brent A. Neuschwander-Tetri, MD acquisition of data drafting of manuscript critical revision of manuscript for important intellectual content
Arun Sanyal, MD acquisition of data drafting of manuscript critical revision of manuscript for important intellectual content
Rohit Loomba, MD, MHSc study concept and design acquisition of data analysis and interpretation of data drafting of manuscript critical revision of manuscript for important intellectual content study supervision
Claude B. Sirlin, MD study concept and design acquisition of data analysis and interpretation of data drafting of manuscript critical revision of manuscript for important intellectual content study supervision obtaining funding
for the NASH Clinical Research Network study concept and design technical support administrative support

[1]Department of Radiology, UCSD School of Medicine, San Diego, California [2]Department of Radiology, Duke University Medical Center, 3808, Durham, North Carolina [3]Saint Louis University School of Medicine, St. Louis, Missouri [4]Department of Radiology, Indiana University School of Medicine, Indianapolis, Indiana [5]Laboratory of Pathology, National Cancer Institute [6]Liver Diseases Section, Digestive Diseases Branch, National Institute of Diabetes and Digestive and Kidney Diseases [7]Johns Hopkins Bloomberg School of Public Health, Baltimore, Maryland [8]Division of Pediatric Gastroenterology, Hepatology and Nutrition, Department of Pediatrics, Columbia University Medical Center, New York, New York [9]Virginia Commonwealth University School of Medicine, Richmond, Virginia [10]NAFLD Translational Research Unit, Division of Gastroenterology, UCSD School of Medicine, San Diego, California

Abstract

Background & Aims—We assessed the diagnostic performance of magnetic resonance imaging (MRI) proton density fat fraction (PDFF) in grading hepatic steatosis and change in hepatic steatosis in adults with nonalcoholic steatohepatitis (NASH) in a multi-center study, using central histology as reference.

Methods—We collected data from 113 adults with NASH participating in a multi-center, randomized, double-masked, placebo-controlled, phase 2b trial to compare the efficacy cross-sectionally and longitudinally of obeticholic acid vs placebo. Hepatic steatosis was assessed at baseline and after 72 weeks of obeticholic acid or placebo by liver biopsy and MRI (scanners from different manufacturers, at 1.5T or 3T). We compared steatosis estimates by PDFF vs histology. Histologic steatosis grade was scored in consensus by a pathology committee. Cross-validated receiver operating characteristic (ROC) analyses were performed.

Results—At baseline, 34% of subjects had steatosis grade 0 or 1, 39% had steatosis grade 2, and 27% had steatosis grade 3; corresponding mean PDFF values were 9.8%±3.7%, 18.1%±4.3%, and 30.1%±8.1%. PDFF classified steatosis grade 0–1 vs 2–3 with an area under the ROC curve (AUROC) of 0.95 (95% CI, 0.91–0.98), and grade 0–2 vs grade 3 steatosis with an AUROC of 0.96 (95% CI, 0.93–0.99). PDFF cut-off values at 90% specificity were 16.3% for grades 2–3 and 21.7% for grade 3, with corresponding sensitivities of 83% and 84%. After 72 weeks' of obeticholic vs. placebo, 42% of subjects had a reduced steatosis grade (mean reduction in PDFF from baseline of 7.4%±8.7%), 49% had no change in steatosis grade (mean increase in PDFF from baseline of 0.3%±6.3%), and 9% had an increased steatosis grade (mean increase in PDFF from baseline of 7.7%±6.0%). PDFF change identified subjects with reduced steatosis grade with an AUROC of 0.81 (95% CI, 0.71–0.91) and increased steatosis grade with an AUROC of 0.81 (95% CI, 0.63–0.99). A PDFF reduction of 5.15% identified subjects with reduced steatosis grade with 90% specificity and 58% sensitivity, whereas a PDFF increase of 5.6% identified those with increased steatosis grade with 90% specificity and 57% sensitivity.

Conclusions—Based on data from a phase 2 randomized controlled trial of adults with NASH, PDFF estimated by MRI scanners of different field strength and at different sites, accurately classifies grades and changes in hepatic steatosis when histologic analysis of biopsies is used as a reference.

Keywords

FLINT; NAFLD; direct comparison; non-invasive

Introduction

Nonalcoholic fatty liver disease (NAFLD) is estimated to affect a billion people in the world today [1,2]. Reported population-based prevalence estimates of nonalcoholic steatohepatitis (NASH), in which hepatocellular injury and inflammation are present in addition to steatosis, have ranged from 1.1% to 18.5% [3], with even larger percentages for higher-risk subpopulations [4,5]. Long-term outcomes of patients diagnosed with NASH include diabetes, cardiovascular disease, cirrhosis, hepatocellular carcinoma, and death [6,7].

Magnetic resonance imaging (MRI)-estimated proton density fat fraction (PDFF) is a non-invasive biomarker of hepatic steatosis, which is a key feature of NAFLD and NASH [8]. In single-site cross-sectional studies, PDFF has been shown to be accurate using magnetic resonance spectroscopy (MRS) as a reference standard [9,10,11,12], and to be reproducible across scanner manufacturers and field strengths [13,14]. Moreover, other single-center cross-sectional studies using liver biopsy as reference have shown that PDFF correlates with hepatic steatosis grade [15,16,17,18,19], and accurately classifies dichotomized steatosis grade with areas under receiver operating characteristic (ROC) curves ranging from 0.825 to 0.989 [15,20]. The performance of PDFF as a biomarker for hepatic steatosis has also been investigated in single-center longitudinal treatment trials. In the MOZART trial (35 subjects, diagnosed NASH, treated with ezetimibe vs placebo for 24 weeks), histologic responders (reduction in NAFLD Activity Score [NAS] of two or more points) had greater relative PDFF reduction (29.3%) than non-responders (2.0%) [21]. In another randomized trial (34 subjects, diagnosed NASH, treated with N-3 fish oil vs placebo for one year), subjects treated with N3 lost more weight and showed a greater decrease in PDFF than those treated with placebo, although there were no differences in histologic response [22]. Until now, however, diagnostic performance of PDFF has not been investigated in a well-controlled, multi-center treatment trial. Assessing multi-center diagnostic performance is necessary to further validate PDFF prior to its widespread adoption and implementation [20].

Therefore, the purpose of this study was to assess cross-sectional and longitudinal diagnostic performance of PDFF to grade hepatic steatosis in adults using centrally-scored histology as reference. To do this, we performed a prospectively-designed study of PDFF estimated by MRI in the Farnesoid X Receptor Ligand Obeticholic Acid in NASH Treatment (FLINT) trial [23]. The FLINT trial was a multi-center, randomized, double-masked, placebo-controlled, phase 2b clinical trial of treatment with either obeticholic acid or placebo in patients with NASH. Hepatic steatosis was assessed at baseline and after 72 weeks of obeticholic acid vs placebo by both liver biopsy and MRI, allowing comparison of PDFF to histologic hepatic steatosis grade in a well-characterized, longitudinal multi-center study.

Materials and Methods

Study design

MRI was offered at baseline and end-of-treatment (EOT) to adults participating in the FLINT trial. PDFF was a secondary imaging endpoint, for which histologic hepatic steatosis grade served as the reference standard.

Eligibility criteria for the FLINT trial are published elsewhere [23]; all subjects were diagnosed with NASH based on local histology review of a standard-of-care liver biopsy. Inclusion criteria for the liver MRI portion of the FLINT trial were that the subject was enrolled, and that the subject was willing and able to complete both MRI exams (the baseline exam prior to randomization and within 90 days of baseline biopsy, and the EOT MRI exam within 90 days of EOT biopsy). MRI exclusion criteria were contraindication to MRI, extreme claustrophobia, pregnancy or trying to become pregnant, weight or girth exceeding MRI scanner capability, or any condition or circumstance that, in the opinion of the clinical trial site investigator would interfere with completion of the MRI exam.

The FLINT trial, including the MRI portion, was approved by an Institutional Review Board at each participating clinical trial site, and was in compliance with the Health Insurance Portability and Accountability Act. All subjects enrolled in the FLINT trial signed informed consent for MRI exams.

All authors had access to the study data and have reviewed and approved the final manuscript.

MRI clinical trial site qualification

The MRI portion of this study was managed by the NASH CRN Radiology Coordinating Center (RCC) in conjunction with the NASH CRN Data Coordinating Center (DCC). The RCC ensured that each participating clinical trial site was qualified to participate in the MRI portion of the FLINT trial based on submission of technically adequate phantom or volunteer MRI data, and provided central imaging quality control.

MRI exams

Seven of the eight participating FLINT clinical trial sites contributed MRI data to this study using 1.5T (three sites) and 3T (four sites) MR scanners (Table 1). At six of the seven clinical trial sites, a single scanner was used so that longitudinal instrument-dependent measurement variability was minimized; at the seventh site (Site E) two scanners from the same manufacturer and of the same field strength, but of different model type were used. PDFF reproducibility has been demonstrated in two studies across different clinical trial sites, and for both field strengths used in this study [13,14].

For each MRI exam, an advanced, non-contrast, breath-hold, magnitude-based, gradient-recalled-echo (GRE), two-dimensional axial sequence was obtained of the entire liver using a torso array coil centered over the liver. T1 effects that could cause subject- or scanner-dependent bias were minimized using a low flip angle (ten degrees) and a repetition time (TR) of ≥ 120 ms. Six echoes were collected at alternately out-of-phase and in-phase echo

times (TEs) for the water and main fat peaks to permit PDFF quantification while accounting for subject-based T2* effects [9,10,11,12] (Table 1). Images in Digital Imaging and Communications in Medicine (DICOM) format were transferred from clinical trial sites to the RCC for analysis.

MRI analysis

Data analysts at the RCC placed one circular 1-cm radius region of interest (ROI) on 5th echo (out-of-phase) images in each of the nine anatomical liver segments; those ROIs were propagated to images for the other echoes. Mean signal intensities at those ROI locations were recorded. A custom MATLAB™ (The MathWorks, Natick, MA, USA) multi-peak, non-linear, least-squares fitting algorithm [9,10,11,12] that accounted for T2* signal decay and multi-frequency interference effects of the various proton locations in triglyceride [24] was used to estimate PDFF for each ROI location.

Liver biopsy

Percutaneous core liver biopsies were performed by NASH CRN investigators as research procedures or for clinical care. Hematoxylin and eosin (H&E), Masson's trichrome, and iron stains were prepared from formalin-fixed tissue specimens. The interval between performance of MRI and biopsy was calculated. Local clinical trial site histological analysis was performed to determine eligibility for FLINT trial enrollment; those local scores were not used in the current analysis.

Comparison of histologic steatosis grade and PDFF

PDFF, and histologic steatosis percentage (and grade) both assess liver fat, but they do so in very different ways. Histologic steatosis assessment yields a percentage of hepatocytes that show fat globules on H&E stain (from whence is derived a steatosis grade from 0 to 3), whereas PDFF estimates a ratio of observable MRI signal from fat, compared to all observable MRI signal (from both fat and water). Thus, if all examined hepatocytes were seen to be filled with 50% fat globules, the histologic steatosis percentage would be 100% since all cells show fat globules, and the steatosis grade would be 3, but the MRI PDFF percentage would be, ignoring technical factors for the moment, something like 50%. Thus, we see in practice that PDFF percentages typically are somewhat less than half of histologic steatosis percentages.

Central histological analysis

Biopsies were reviewed by the pathologists of the NASH CRN Pathology Committee who provided central histology assessment by consensus at a multi-head microscope. Pathologists were blinded to all clinical information, including participation in this study. Steatosis grade was provided according to the standardized NASH CRN histological NAFLD scoring system (proportion of hepatocytes containing fat macrovesicles: grade 0 for < 5%, grade 1 for 5 to 33%, grade 2 for > 33 to 66%, and grade 3 for > 66% [25]). Other centrally scored features that were evaluated in this study were lobular inflammation, portal inflammation, hepatocellular ballooning, fibrosis stage, and NAFLD Activity Score (NAS).

Blinding

RCC analysts and other staff at the RCC were blinded to histology results, and pathologists were blinded to imaging results. RCC analysts were blinded to treatment assignment.

Other data

Subject demographics, laboratory, anthropomorphic measurements, and medical history were collected at each clinical trial site.

Statistical analysis

Statistical analyses were done with SAS (SAS Institute 2011, Base SAS 9·3 Procedures Guide) and Stata (StataCorp 2013, Stata Statistical Software: release 13).

A single PDFF value was calculated for each MRI exam as the mean of the PDFF values for the nine anatomical liver segments. Demographic, histologic and imaging information were summarized with categorical variables expressed as numbers and percentages and continuous variables expressed by mean (± standard deviation [SD]). The proportion of subjects who had, vs did not have MRIs at baseline was compared with regard to treatment group, study site, demographics, liver enzymes, lipids, metabolic factors, co-morbidities, concomitant liver medications, and histology findings. Pearson partial correlation coefficients and 95% confidence intervals were estimated between PDFF and histologic variables (steatosis, lobular inflammation, hepatocellular ballooning, fibrosis, and portal inflammation) at baseline and for changes from baseline to 72 weeks.

Diagnostic accuracy of PDFF to classify hepatic steatosis grade at baseline was tested for grades 0-1 vs 2-3, and grades 0-2 vs 3. Diagnostic accuracy of change in PDFF to classify change in hepatic steatosis grade from baseline to EOT was tested for: reduction vs no change/increase and increase vs no change/decrease. Cross-validated area under ROC (AUROC) curves using a jack-knife procedure and 95% CIs were estimated for each of these dichotomizations [26]. Cut-off PDFF values were estimated using the lowest threshold value for which there was ≥ 90% specificity to distinguish between these dichotomized categories. Sensitivity, positive predictive values (PPVs), and negative predictive valves (NPVs) were calculated along with 95% confidence intervals (CIs) fixing specificity at 90%.

Results

Of 283 adults enrolled in the FLINT trial from March 16, 2011 to December 3, 2012 at eight participating FLINT clinical trial sites, 113 (40%) had MRI and liver biopsy at baseline, 85 (30%) had MRI and liver biopsy at EOT, and 78 (28%) had MRI and liver biopsy at both time points. One subject with a baseline MRI but without a centrally-read baseline liver biopsy was excluded from the analysis. All baseline MRIs were performed prior to randomization and occurred an average of 51 days following baseline biopsy. Follow-up MRIs were performed an average of two days after follow-up biopsy, and were performed from 29 days before to 78 days after biopsy.

Cohort baseline population characteristics are summarized in Table 2. Subjects who had, vs did not have MRIs had significantly ($p < 0.05$) lower mean aspartate aminotransferase,

alkaline phosphatase, weight, BMI and prevalence of hyperlipidemia and hypertension. Additionally, the 78 subjects with both paired MRIs and paired biopsies vs the 204 subjects without, had lower ($p < 0.05$) mean AST, ALT and alkaline phosphatase at baseline.

Cross-sectional analysis

The distribution of PDFF at baseline is shown in Figure 1: PDFF mean was 18.6%±9.6%, and ranged from 3.7% to 49.3%.

At baseline, 34% (38/113) of biopsies had steatosis grade 0 or 1, 39% (44/113) had grade 2, and 27% (31/113) had grade 3 with corresponding mean PDFF values of 9.8%±3.7%, 18.1% ±4.3%, and 30.1%±8.1%, respectively. PDFF values for each histologic steatosis grade at baseline are shown in Figure 2. Higher steatosis grade corresponded to higher mean PDFF.

Partial correlation of baseline PDFF values with histologic features is summarized in Table 3. PDFF is highly correlated with steatosis controlling for other histologic features (Pearson Partial Correlation = 0.80 [95% CI, 0.73–0.86]; $p < 0.001$).

Diagnostic accuracy of PDFF for classifying steatosis is summarized in Table 4. The area under ROC (AUROC) from logistic regression using PDFF as a surrogate for classifying steatosis grade 0-1 vs 2-3 was 0.95 (95% CI, 0.91–0.98) and for classifying steatosis grade 0-2 vs 3 was 0.96 (95 % CI, 0.93–0.99). PDFF cut-off values at 90% specificity were 16.3% for grades 2-3, and 21.7% for grade 3 discrimination. Diagnostic accuracy of PDFF for classifying steatosis was similar between the 1.5T vs. 3T scanners (data not shown).

Longitudinal analysis

PDFF values for each histologic hepatic steatosis grade change category (reduction, no change, and increase in steatosis grade) are shown in the box plots in Figure 3. Changes in PDFF were positive in 71% (5/7) of subjects in whom steatosis grade increased and were negative in of subjects in 91% (30/33) of subjects in whom steatosis grade decreased. The mean (SD) change in MRI-PDFF in 38 subjects with no change in histology grade category was 0.3%±6.3%, ranging from −21.1 to +21.0%.

Correlation of change from baseline to EOT in PDFF values with change from baseline to EOT in histologic features is summarized in Table 3. Correlation between change in PDFF and change in histologic steatosis grade controlling for other histologic features was high (Pearson Partial Correlation = 0.63 [95% CI, 0.47–0,75]; $p < 0.001$).

Diagnostic accuracy of change in PDFF vs change in histologic hepatic steatosis grade from baseline to EOT is summarized in Table 4. At EOT, 42% of paired biopsies had improvement in steatosis grade, 49% had no change, and 9% had worsening. The AUROC using PDFF change to classify histologic hepatic steatosis grade improvement and worsening, respectively, were 0.81 (95% CI, 0.71–0.91) and 0.81 (95% CI, 0.63–0.99). Cut-off values for PDFF change at 90% specificity were −5.1% for improvement and +5.6% for worsening hepatic steatosis grade.

Discussion

We compared PDFF to histologic hepatic steatosis grade at baseline, and change in PDFF to change in histologic hepatic steatosis grade from baseline to EOT. We found that PDFF correlates well with histologic hepatic steatosis grade cross-sectionally, and that change in PDFF correlates well with change in histologic hepatic steatosis grade longitudinally.

ROC analysis at baseline yielded PDFF cutoffs predicting histologic hepatic steatosis grade that are similar to those reported in the literature for a single-center study. We found that at 90% specificity, PDFF cut-off values were 16.3% (83% sensitivity) and 21.7% (84% sensitivity) for discrimination of histologic steatosis grades 0-1 from 2-3, and grades 0-2 from 3, respectively. Tang et al [15] reported PDFF cut-off values for those discriminations in their single-center study of 77 children and adults with known or suspected NAFLD of 17.4% (64% sensitivity and 96% specificity) and 22.1% (71% sensitivity and 92% specificity), respectively. In a subsequent single-center study of 89 adults, Tang et al [27] subsequently reported high sensitivity and specificity for those cutoffs to distinguish steatosis grades in another clinical trial. As emphasized previously by others [28], PDFF is a quantitative marker of MRI-visible fat content while histology scoring is a semi-quantitative marker of proportion of steatotic hepatocytes. Since PDFF and histology do not attempt to measure the same quantity, perfect agreement is not expected.

The AUROC of PDFF for classifying longitudinal change in steatosis is 0.81, which is inferior to its cross-sectional performance at baseline. The lower AUROC for change may reflect the ‘noisiness’ of histologic grading as a marker of steatosis, an effect which is amplified when differences in PDFF are compared to differences in histologic steatosis grade.

Hepatic steatosis may also be assessed non-invasively by CAP (a transient elastography-derived controlled attenuation parameter), which is an estimate of total ultrasound attenuation [29]. Although we did not perform a direct comparison of CAP and PDFF, the accuracy of MRI to estimate PDFF has been reported to be higher than that of CAP, using histology as reference standard [30 31].

Strengths of this study are that the cohort of patients that was studied was well-characterized, with a racial/ethnic makeup representative of patients diagnosed with NASH in the United States; that subjects enrolled in this study had both pre- and post-treatment biopsy; that histology was scored centrally by the NASH CRN Pathology Committee; and that a range of MRI scanner manufacturers at two field strengths and across multiple study sites were utilized. Thus, our study results are likely to be generalizable to the entire adult NASH population in the United States, while also providing compelling evidence that MRI-PDFF can be applied successfully in multi-center trials.

A major limitation of this study was that not all subjects enrolled in the FLINT trial had MRIs. Only 40% of randomized subjects had an MRI at baseline and only 28% had paired EOT and baseline MRIs. Participation in the MRI study was reduced because the MRI qualification process at each clinic was completed after the start of enrollment into the trial. Participation rates into the MRI study varied widely at the eight study sites, ranging from 0

to 84%. In addition, subjects who had the MRI weighed significantly less than those who did not participate; this may be because the heaviest FLINT participants were too large to undergo MRI. Also, significantly lower mean alanine aminotransferase and aspartate aminotransferase and lower rates of hyperlipidemia and hypertension were seen at baseline in those who did vs did not participate in the MRI study suggesting a less severe group in those who participated. Our results could be biased if the relationships between MRI-PDFF and histologic features varied in those who participated vs did not participate in the MRI study.

Another limitation was that relatively few subjects of non-White race were included. This was unavoidable since NASH is relatively uncommon in non-Whites, and the racial and ethnic diversity of our study population reflects that seen in the national prevalence of NASH. Our study also did not include children, as the FLINT trial enrolled only adults; thus multi-center validation studies of MRI PDFF in children are needed. Finally, potentially confounding factors such as those in Table 2 were not investigated because the study was not powered to permit those investigations. It is also not likely that there are meaningful confounders to our results, given that none have been reported for single-site studies [14,15].

Steatosis grade was determined in this study according to the standardized NASH CRN histological NAFLD scoring system based on the proportion of hepatocytes containing fat macrovesicles. The performance of MRI PDFF compared to microvesicular steatosis remains unclear, especially since microvesicular steatosis is often under-staged. The relationship of microvesicular steatosis and PDFF was not examined in this paper because all work to date validating MRI PDFF against MR spectroscopy and histology has considered only macrovesicular steatosis, and because microvesicular steatosis is an uncommon finding in NASH tending to be seen in the more severe cases [32].

Finally, since an inclusion criterion for the FLINT trial was the presence of NASH as assessed by a local pathologist, only one subject had histologic hepatic steatosis grade 0 at central reading. Hence, grades 0 and 1 were considered as a single category in our analyses. Further multi-center studies in populations including subjects with lower amounts of hepatic steatosis (i.e., grades 0 and 1) are needed to investigate correlations of PDFF with hepatic steatosis in that range.

In conclusion, in a well-controlled, multi-center study in adults, PDFF showed high agreement with histologic hepatic steatosis grade based on MRI data at sites using scanners from different manufacturers and of different field strengths. Importantly, change in PDFF accurately classified change in EOT histologic hepatic steatosis grade. These findings support wider use of PDFF in multi-center trials in adults as a biomarker for hepatic steatosis at baseline, and for change in hepatic steatosis with treatment.

Acknowledgments

We would like to express our appreciation to all of the patients who participated in this study, as well as to the staff of the NASH CRN Data Coordinating Center, the UCSD Radiology Coordinating Center, and all of the participating clinical centers for their support and assistance in conducting this study.

Funding

We would like to acknowledge support from the following sources: NIDDK U01 DK061718, U01 DK061728, U01 DK061731, U01 DK061732, U01 DK061734, U01 DK061737, U01 DK061738, U01 DK061730, and U01 DK061713; NCATS UL1 TR000439, UL1 TR000436, UL1 TR000006, UL1 TR000448, UL1 TR000100, UL1 TR000004, UL1 TR000423, and UL1 TR000058); NCI.

References

1. Machado MV, Cortez-Pinto H. Non-alcoholic fatty liver disease: What the clinician needs to know. World J Gastroenterology. 2014; 20:12956–12980.
2. Loomba R, Sanyal AJ. The global NAFLD epidemic. Nat Rev Gastroenterol Hepatol. 2013; 10:686–690. [PubMed: 24042449]
3. Wanless IR, Lentz JS. Fatty liver hepatitis (steatohepatitis) and obesity: an autopsy study with analysis of risk factors. Hepatology. 1990; 12:1106–1110. [PubMed: 2227807]
4. Lazo M, Clark JM. The epidemiology of nonalcoholic fatty liver disease: a global perspective. Semin Liv Dis. 2008; 28:339–350.
5. Machado M, Marques-Vidal P, Cortez-Pinto H. Hepatic histology obese patients undergoing bariatric surgery. J Hepatol. 2006; 45:600–606. [PubMed: 16899321]
6. Williams CD, Stengel J, Asike MI, et al. Prevalence of nonalcoholic fatty liver disease and nonalcoholic steatohepatitis among a largely middle-aged population utilizing ultrasound and liver biopsy: a prospective study. Gastroenterology. 2011; 140:124–131. [PubMed: 20858492]
7. LaBrecque DR, Abbas Z, Anania F, et al. World Gastroenterology Organisation global guidelines: Nonalcoholic fatty liver disease and nonalcoholic steatohepatitis. J Clin Gastroenterology. 2014; 48:467–473.
8. Schwimmer JB, Middleton MS, Deutsch R, Lavine JE. A phase 2 clinical trial of metformin as a treatment for non-diabetic paediatric non-alcoholic steatohepatitis. Aliment Pharmacol Ther. 2005; 21:871–879. [PubMed: 15801922]
9. Bydder M, Yokoo T, Hamilton G, et al. Relaxation effects in the quantification of fat using gradient echo imaging. Magnetic Resonance Imaging. 2008; 26:347–359. [PubMed: 18093781]
10. Yokoo T, Collins JM, Hanna RF, et al. Effects of intravenous gadolinium administration and flip angle on the assessment of liver fat signal fraction with opposed-phase and in-phase imaging. Journal of Magnetic Resonance Imaging. 2008; 28:246–251. [PubMed: 18581393]
11. Yokoo T, Bydder M, Hamilton G, et al. Nonalcoholic fatty liver disease: diagnostic and fat-grading accuracy of low-flip-angle multiecho gradient-recalled-echo MR imaging at 1.5 T. Radiology. 2009; 251:67–76. [PubMed: 19221054]
12. Yokoo T, Shiehmorteza M, Hamilton G, et al. Estimation of Hepatic Proton-Density Fat Fraction by Magnetic Resonance Imaging at 3T. Radiology. 2011; 258:749–759. [PubMed: 21212366]
13. Kang GH, Cruite I, Shiehmorteza M, et al. Reproducibility of MRI-determined proton density fat fraction across two different MR scanner platforms. Journal of Magnetic Resonance Imaging. 2011; 34:928–934. [PubMed: 21769986]
14. Negrete LM, Middleton MS, Clark L, et al. Inter-examination precision of magnitude-based magnetic resonance imaging for estimation of segmental hepatic proton density fat fraction (PDFF) in obese subjects. Journal of Magnetic Resonance Imaging. 2013; 39:1265–1271. [PubMed: 24136736]
15. Tang A, Tan J, Sun M, et al. Nonalcoholic fatty liver disease: MR imaging of liver proton density fat fraction to assess hepatic steatosis. Radiology. 2013; 267:422–431. [PubMed: 23382291]
16. Permutt Z, Le TA, Peterson MR, et al. Correlation between liver histology and novel magnetic resonance imaging in adult patients with non-alcoholic fatty liver disease - MRI accurately quantifies hepatic steatosis in NAFLD. Aliment Pharmacol Ther. 2012; 36:22–29. [PubMed: 22554256]
17. Le TA, Chen J, Changchien C, et al. Effect of colesevelam on liver fat quantified by magnetic resonance in nonalcoholic steatohepatitis: a randomized controlled trial. Hepatology. 2012; 56:922–932. [PubMed: 22431131]

18. Noureddin M, Lam J, Peterson MR, et al. Utility of magnetic resonance imaging versus histology for quantifying changes in liver fat in nonalcoholic fatty liver disease trials. Hepatology. 2013; 58:1930–1940. [PubMed: 23696515]
19. Loomba R, Sirlin CB, Ang B, et al. Ezetimibe for the treatment of nonalcoholic steatohepatitis: assessment by novel magnetic resonance imaging and magnetic resonance elastography in a randomized trial (MOZART trial). Hepatology. 2015; 61:1239–1250. [PubMed: 25482832]
20. Tang A, Desai A, Hamilton G, et al. Accuracy of MR imaging-estimated proton density fat fraction for classification of dichotomized histologic steatosis grades in nonalcoholic fatty liver disease. Radiology. 2015; 274:416–425. [PubMed: 25247408]
21. Patel J, Bettencourt R, Cui J, et al. Association of noninvasive quantitative decline in liver fat content on MRI with histologic response in nonalcoholic steatohepatitis. Therap Adv Gastroenterol. 2016; 9:692–701.
22. Argo CK, Patrie JT, Lackner C, et al. Effects of n-3 fish oil on metabolic and histological parameters in NASH: a double-blind, randomized, placebo-controlled trial. J Hepatol. 2015; 62:190–197. [PubMed: 25195547]
23. Neuschwander-Tetri BA, Loomba R, Sanyal AJ, et al. Farnesoid X nuclear receptor ligand obeticholic acid for non-cirrhotic, non-alcoholic steatohepatitis (FLINT): a multicentre, randomised, placebo-controlled trial. Lancet. 2015; 385:956–965. [PubMed: 25468160]
24. Hamilton G, Yokoo T, Bydder M, et al. In vivo Characterization of the Liver Fat 1H Magnetic Resonance Spectrum. NMR Biomedicine. 2011; 24:784–790.
25. Kleiner DE, Brunt EM, Van Natta M, et al. Nonalcoholic steatohepatitis clinical research network. Design and validation of a histological scoring system for nonalcoholic fatty liver disease. Hepatology. 2005; 41:1313–1321. [PubMed: 15915461]
26. Lachenbruch P, Mickey M. Estimation of error rates in discriminant analysis. Technometrics. 1968; 10:1–11.
27. Tang A, Desai A, Hamilton G, et al. Accuracy of MR imaging-estimated proton density fat fraction for classification of dichotomized histologic steatosis grades in nonalcoholic fatty liver disease. Radiology. 2015; 274:416–425. [PubMed: 25247408]
28. Bonekamp S, Tang A, Mashhood A, et al. Spatial distribution of MRI-determined hepatic proton density fat fraction in adults with nonalcoholic fatty liver disease. J Magn Reson Imaging. 2014; 39:1525–1532. [PubMed: 24987758]
29. Sasso M, Beaugrand M, de Ledinghen V, et al. Controlled attenuation parameter (CAP): a novel VCTE guided ultrasonic attenuation measurement for the evaluation of hepatic steatosis: preliminary study and validation in a cohort of patients with chronic liver disease from various causes. Ultrasound Med Biol. 36:1825–1835.
30. Imajo K, Kessoku T, Honda Y, et al. Magnetic resonance imaging more accurately classifies steatosis and fibrosis in patients with nonalcoholic fatty liver disease than transient elastography. Gastroenterology. 2016; 150:626–637. [PubMed: 26677985]
31. Taouli B, Serfaty L. Magnetic resonance imaging/elastography is superior to transient elastography for detection of liver fibrosis and fat in nonalcoholic fatty liver disease (editorial). Gastroenterology. 2016; 150:553–556. [PubMed: 26820053]
32. Tandra S, Yeh MM, Brunt EM, et al. Presence and significance of microvesicular steatosis in nonalcoholic fatty liver disease. J Hepatol. 2011; 55:654–659. [PubMed: 21172393]

Abbreviations

AUROC	area under receiving operating curve
BMI	body mass index
CAP	NAFLD activity score
CI	confidence interval

CRN	clinical research network
DCC	Data Coordinating Committee
DICOM	Digital Imaging and Communications in Medicine
EOT	end of treatment
FLINT	Farnesoid X Receptor Ligand Obeticholic Acid in NASH Treatment Trial
GRE	gradient-recalled echo
H&E	Hematoxylin and eosin
MRI	magnetic resonance imaging
MRS	magnetic resonance spectroscopy
NAS	NAFLD activity score
NAFLD	nonalcoholic fatty liver disease
NASH	nonalcoholic steatohepatitis
NPV	negative predictive value
PDFF	proton density fat fraction
PPD	positive predictive value
ROC	receiver operating characteristic
SD	standard deviation
RCC	Radiology Coordinating Center
ROI	region of interest
TE	time to echo
TR	repeat time

Disclosures

Michael S. Middleton, MD PhD Alexion (Contracted work through university, through Biomedical Systems as CRO)

AstraZeneca (Contracted work through university, through Profil as CRO)

Bioclinica (Contracted work through university Genzyme/Sanofi as sponsor)

Biomedical Systems (Contracted work through university)

Bracco (Consultant)

Bristol-Myers Squibb (Contracted work through university)

Celgene (CDA to discuss contracted work through university)

Galmed (Contracted work through university)

Genentech (CDA to discuss contracted work through university)

General Electric (Stockholder, contracted work through university, grant)

Genzyme (Contracted work through university)

Gilead (Grant, and contracted work through university)

Guerbet (Grant)

Icon (CDA to discuss contracted work through university)

Intercept Pharmaceuticals (Contracted work through university)

Isis (Contracted work through university)

Janssen (Contracted work through university)

Merge Healthcare (Consultant)

NuSirt (Contracted work through university)

Perspectum (CDA to discuss contracted work through university)

Pfizer (Contracted work through university, stockholder)

Profil (Contracted work through university, for sponsor AstraZeneca)

Quantitative Insights (Consultant)

Sanofi (Contracted work through university)

Shire (CDA with Icon, with Shire as sponsor, to discuss contracted work through university)

Siemens (Contracted work through university)

Synageva (Contracted work through university, through Biomedical Systems as CRO)

Takeda (Contracted work through university)

Virtualscopics (Contracted work through university)

Zydus (Discussions leading to CDA to discuss contracted work through university)

Elhamy R. Heba, MD no COI

Catherine A. Hooker, BSc no COI

Mustafa Bashir, MD RadMD (Consultant)

Siemens Healthcare (Research grant)

NGM Biopharmaceuticals (Research grant)

TaiwanJ Pharmaceuticals (Research grant)

Kathryn J. Fowler, MD no COI

Kumar Sandrasegaran, MD no COI

Elizabeth M. Brunt, MD no COI

David E. Kleiner, MD PhD no COI

Edward Doo, MD no COI

Mark L. Van Natta, MHS no COI

James Tonascia, PhD no COI

Joel E. Lavine, MD, PhD no COI

Brent A. Neuschwander-Tetri, MD Nimbus Therapeutics (Consultant)

Enanta (Consultant)

Novartis (Consultant)

Galmed (Consultant)

Zafgen (Consultant)

Receptos (Consultant)

Pfizer (Consultant)

Allergan (Consultant)

MedImmune/AstraZeneca (Consultant)

Arun Sanyal, MD AbbVie (Consultant)

Astra Zeneca (Institutional grant support)

Boehringer Ingelhiem (Consultant)

Bristol-Myers Squibb (Institutional grant support)

Astra Zeneca (Consultant)

Echosens (Unpaid consultant)

Eli Lilly (Unpaid consultant)

Exalenz Bioscience (Consultant)

FibroGen (Consultant)

Genfit (Stock options, consultant)

Gilead (Institutional grant support)

Hemoshear (Consultant)

Immune Pharma (Consultant)

Immuron (Consultant)

Intercept Pharmaceuticals (Unpaid consultant)

Merck (Institutional grant support)

Nimbus Therapeutics (Consultant)

Nitto Denko (Consultant)

Novartis (Institutional grant support)

Pfizer (Consultant)

Salix Pharmaceuticals (Consultant, institutional grant support)

Sanyal Biotechnologies (President)

Takeda (Consultant)

Tobira Therapeutics (Consultant, institutional grant support)

Rohit Loomba, MD, MHSc Adheron (Research funding)

Alnylam (Consultant)

Arisaph (Research funding)

Arrowhead Research (Advisory board)

Boehringer Ingelheim (Consultant)

Bristol-Myers Squibb (Research funding, advisory board, consultant)

Celgene (Consultant)

CNI (Consultant)

Conatus (Advisory board, consultant)

Daiichi-Sankyo Inc (Research funding)

DeuteRx (Consultant)

Eli Lilly (Consultant)

Enanta (Consultant)

Fibrogen (Consultant)

Galmed (Research funding, advisory board)

General Electric (Research funding)

Gilead (Research funding, advisory board, consultant)

Immuron (Research funding)

Intercept Pharmaceuticals (Clinical trial steering committee)

Isis (Consultant)

Janssen (Consultant)

Kinemed (Research funding)

Liponexus Inc (Co-founder)

Merck (Research funding, consultant)

Metacrine (Consultant)

MS (Research funding, advisory board, consultant)

NGM Biopharmaceuticals (Research funding, consultant)

Nimbus (Advisory board)

Pfizer (Consultant)

Promedior (Research funding)

Receptos (Consultant)

RuiYi (Consultant)

Scholar Rock (Consultant)

Shire (Consultant)

Siemens (Research funding)

Tobira (Research funding, advisory board)

Viking (Consultant)

Zafgen (Consultant)

Claude B. Sirlin, MD Alexion (Contracted work through university, (through Biomedical Systems as CRO)

AstraZeneca (Contracted work through university, through Profil as CRO)

Bioclinica (Contracted work through university Genzyme/Sanofi as sponsor)

Biomedical Systems (Contracted work through university)

Bracco (Consultant)

Bristol-Myers Squibb (Contracted work through university)

Fibrogen (Consultant)

Galmed (Contracted work through university)

General Electric (Contracted through university, grant)

Genzyme (Contracted work through university)

Gilead (Contracted work through university)

Guerbet (Grant)

Icon (CDA to discuss contracted work through university)

Intercept Pharmaceuticals (CDA to discuss contracted work through university)

Isis (Contracted work through university)

Janssen (Contracted work through university)

NuSirt (Contracted work through university)

Perspectum (CDA to discuss contracted work through university)

Pfizer (Contracted work through university)

Profil (Contracted work through university, for sponsor AstraZeneca)

Sanofi (Contracted work through university)

Shire (CDA with Icon, with Shire as Sponsor, to discuss contracted work through university)

Siemens (Contracted work through university)

Synageva (Contracted work through university, through Biomedical Systems as CRO)

Takeda (Contracted work through university)

Tobira (Consultant)

Virtualscopics (Contracted work through university)

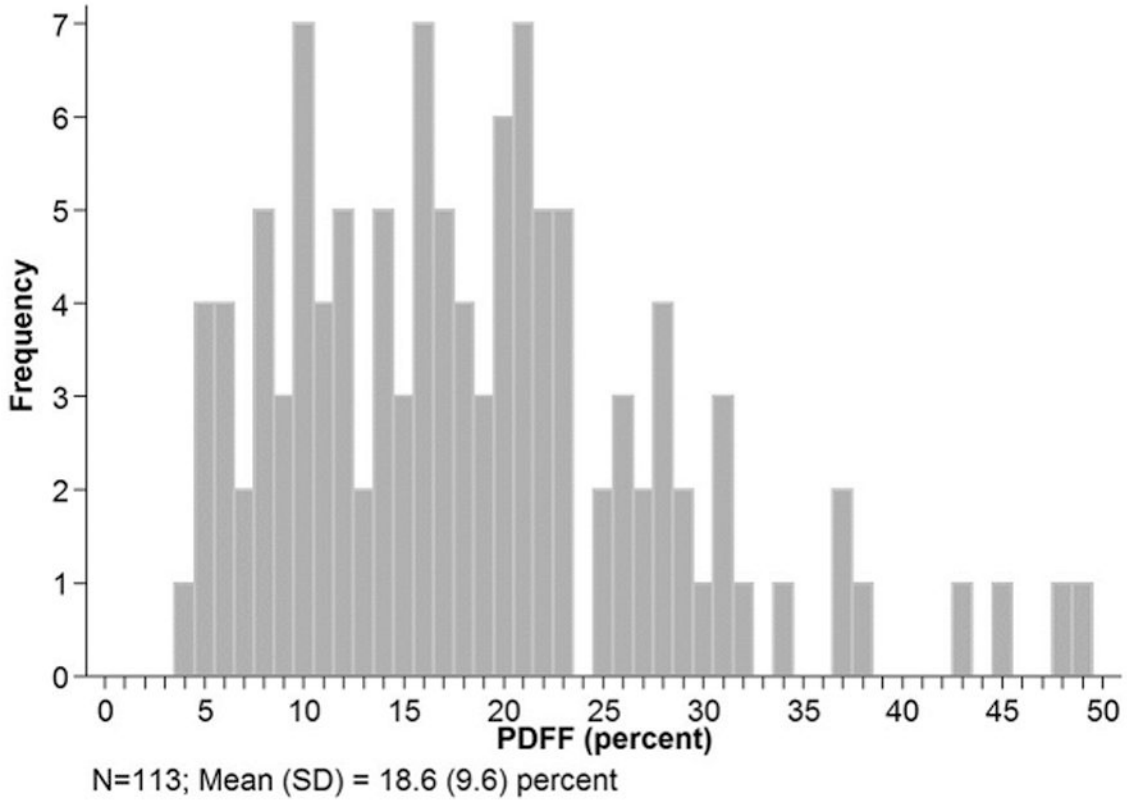

Figure 1.
PDFF distribution of study population at baseline.

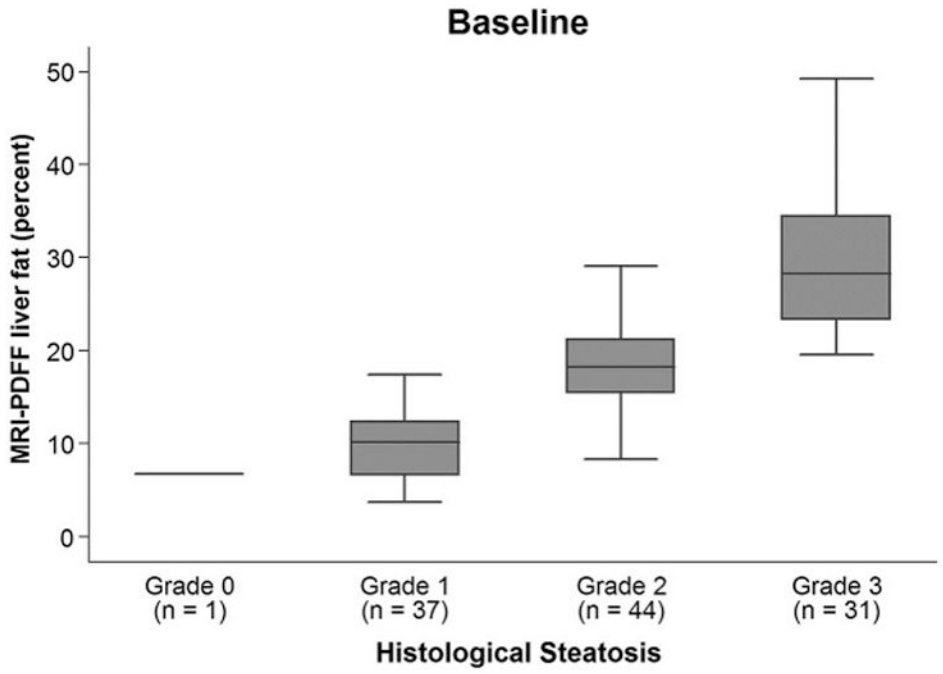

Figure 2.

Bar and whisker plot at baseline of PDFF vs steatosis grade. For each steatosis grade, maximum and minimum PDFF values are indicated by horizontal lines at the bottom and top of each steatosis grade entry, the darkened box in the middle represents PDFF data points in the 25% to 75% interquartile range, and the line through the middle of the central darkened box represents the median PDFF value.

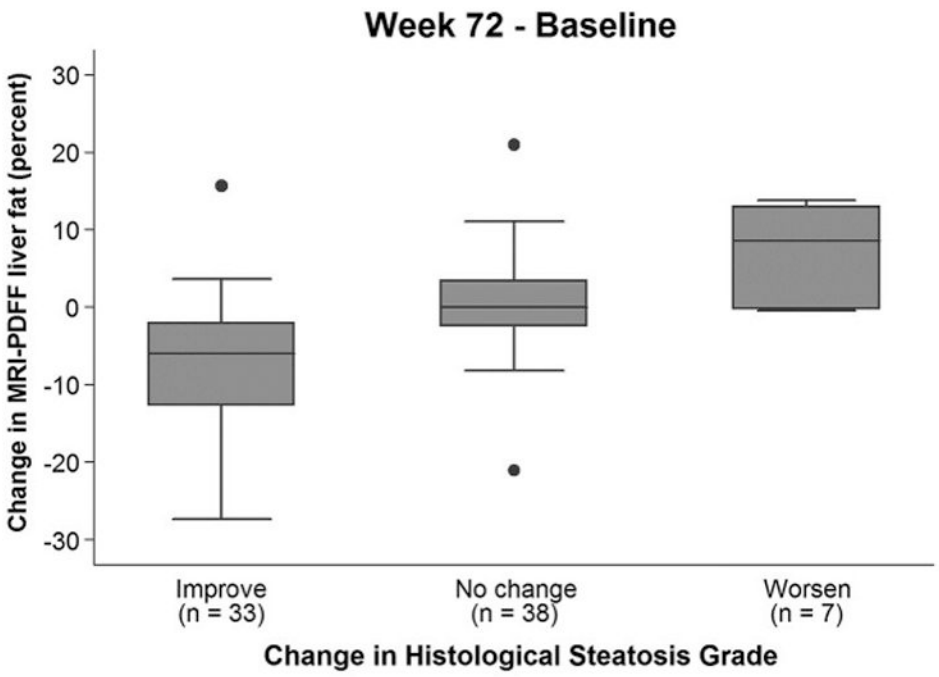

Figure 3.

Bar and whisker plot of change in PDFF vs change in histologic hepatic steatosis grade. Mean PDFF change values for steatosis grade reduction, no change in steatosis grade, and increase in steatosis grade were, respectively: −7.4%± 8.7% (n=42), 0.3%±6.3% (n=49), and 7.7%± 6.0% (n=9). Explanations of each bar-and-whisker plot entry are as noted for Figure 2, except that in this figure values represent PDFF change, the maximum and minimum PDFF change values that are indicated by horizontal lines at the bottom and top of each steatosis grade entry exclude outliers, and the isolated dots represent outliers.

Table 1

MRI scanners and techniques

Clinical trial site MR scanners	**1.5T**	**3T**
Site A	-	Siemens TIM Trio
Site B	-	Siemens TIM Trio
Site C	Siemens Avanto	-
Site D	-	GE Signa HDxt
Site E	-	GE Signa HDxt GE Discovery 750W
Site F	Siemens Avanto	-
Site G	Siemens TIM Symphony	-
Scanning parameters		
Repetition time (ms)	≥ 120	≥ 120
First time-to-echo (ms)	2.3	1.15
Delta time-to-echo (ms)	2.3	1.15
Number of echoes	6	6
Flip angle (°)	10	10
Bandwidth (Hz/Px)	≥ 500	≥ 1,000
Slice thickness (mm)	8 or 10	8 or 10
Slice gap (mm)	0	0
Phase encoding steps	192	128
Frequency encoding steps	192	128

Table 2
Baseline characteristics of those obtaining vs not obtaining baseline MRI

	Baseline MRI (n=113)	No Baseline MRI (n=169)	p-value
Study site * – no.			
Site A	14	15	
Site B	15	12	
Site C	17	10	
Site D	32	6	
Site E	7	21	
Site F	9	33	
Site G	19	18	
Treatment group			
Obeticholic acid – no. (%)	55 (48.7)	86 (50.9)	0.81
Demographics			
Age (yrs)	51±11	51±11	0.98
Male sex -no. (%)	43 (38.0)	53 (31.2)	0.25
White race - no. (%)	93 (82.3)	140 (82.8)	1.00
Hispanic ethnicity - no. (%)	19 (16.8)	24 (14.2)	0.61
Liver enzymes			
Aspartate aminotransferase - U/L	55±32	65±39	**0.03**
Alanine aminotransferase – U/L	76±43	87±54	0.08
γ-Glutamyltransferase – U/L	80±115	75±71	0.71
Alkaline phosphatase - U/L	78±26	85±27	**0.03**
Total bilirubin – mg/dL	0.6±0.3	0.7±0.4	0.49
Metabolic factors			
Weight - kg	95±17	100±23	**0.03**
Body-mass index - kg/m^2	33.6±5.2	35.3±6.9	**0.02**
Waist circumference - cm	109±12	112±16	0.16
Waist to hip ratio	0.95±0.07	0.95±0.09	0.99
Fasting serum glucose - mg/dL	113±31	118±40	0.19
Insulin - umol/mL	28±36	28±27	0.94
HOMA-IR - (mg/dL * umol/mL) / 405	8.5±12.1	8.3±8.7	0.90
Hemoglobin A1c - %	6.3±1.0	6.6±1.1	0.06
Systolic blood pressure - mmHg	130±16	133±16	0.15
Diastolic blood pressure - mmHg	78±11	77±10	0.64
Comorbidities			
Hyperlipidemia - no. (%)	58 (51.3)	115 (68.0)	**0.006**
Hypertension - no. (%)	59 (52.2)	112 (66.3)	**0.02**
Diabetes - no. (%)	57 (50.4)	92 (54.4)	0.54

	Baseline MRI (n=113)	No Baseline MRI (n=169)	p-value
Cardiovascular disease - no. (%)	4 (3.5)	11 (6.5)	0.42
Liver histology findings			
Definite steatohepatitis - no. (%)	91 (80.5)	134 (79.3)	0.88
Fibrosis - stage[1]	1.7±1.1	1.9±1.0	0.23
NAFLD activity score (NAS)[2]	5.2±1.3	5.2±1.3	0.62
Hepatocellular ballooning - score	1.4±0.7	1.4±0.8	0.88
Steatosis - score	1.9±0.8	2.1±0.8	0.08
Lobular inflammation - score	1.8±0.7	1.8±0.7	0.34
Portal inflammation - score[3]	1.1±0.6	1.2±0.6	0.86

Notes: Plus-minus values are means±SD; BMI = body mass index; PDFF = proton density fat fraction; SD = standard deviation.

[*] Two study sites with combined 55 randomized subjects did not obtain MRIs

[1] Fibrosis was assessed on a scale of 0 to 4, with higher scores indicating more severe fibrosis

[2] NAS was assessed on a scale of 0 to 8, with higher scores indicating more severe disease; the components of this measure are steatosis (assessed on a scale of 0 to 3), lobular inflammation (assessed on a scale of 0 to 3), and hepatocellular ballooning (assessed on a scale of 0 to 2)

[3] Portal inflammation was assessed on a scale of 0 to 2 with higher scores indicating more severe inflammation

Table 3

Partial correlation of MRI-PDFF with histologic components at baseline andchange in MRI-PDFF with change in histologic components at EOT

Histologic component	MRI-PDFF at baseline (n=113)			Change in MRI-PDFF at EOT (n=78)		
	r	95% CI	p-value	r	95% CI	p-value
Steatosis	0.80	0.80–0.90	< 0.001	0.63	0.47–0.75	< 0.001
Lobular inflammation	-0.21	-0.28–0.09	0.03	-0.14	-0.36–0.09	0.23
Ballooning	-0.02	-0.51– -0.19	0.85	0.17	-0.06–0.39	0.14
Fibrosis	-0.11	-0.47– -0.14	0.24	-0.18	-0.39–0.05	0.13
Portal inflammation	0.02	-0.30–0.07	0.84	-0.13	-0.35–0.10	0.26

Notes: MRI = magnetic resonance imaging; PDFF = proton density fat fraction; EOT = end of treatment

Table 4

Diagnostic accuracy of PDFF for classifying steatosis

Cross-sectional steatosis grade classification (n=113)	MRI PDFF threshold (%) at 90% specificity		Sensitivity	PPV	NPV	AUROC (95% CI)
0-1 vs 2-3	16.3		83% (62/75)	95% (62/65)	73% (35/48)	0.95 (0.91–0.98)
0-2 vs 3	21.7		84% (26/31)	76% (26/34)	94% (74/79)	0.96 (0.93–0.99)
Longitudinal steatosis grade change classification (n=78)	**Mean (SD) PDFF change (%)**	**Cutoff PDFF change at 90% specificity (%)**	**Sensitivity**	**PPV**	**NPV**	**AUROC (95% CI)**
Decrease in steatosis grade (improvement) (42%)	-7.4±8.7	- 5.1	58% (19/33)	83% (19/23)	75% (41/55)	0.81 (0.71–0.91)
No change in steatosis grade (49%)	0.3±6.3	-	-	-	-	-
Increase in steatosis grade (worsening) (9%)	7.7±6.0	5.6	57% (4/7)	36% (4/11)	96% (64/67)	0.81 (0.63–0.99)

Notes: PDFF = proton density fat fraction; MRI = magnetic resonance imaging; PPV = positive predictive value; NPV = negative predictive value; AUROC = area under ROC curve; CI = confidence interval